Supramolecular Chemistry

International Edition: DOI: 10.1002/anie.201916058
German Edition: DOI: 10.1002/ange.201916058

Strong, Self-Healable, and Recyclable Visible-Light-Responsive Hydrogel Actuators

*Zhen Jiang, Ming Li Tan, Mahdiar Taheri, Qiao Yan, Takuya Tsuzuki, Michael G. Gardiner, Broden Diggle, and Luke A. Connal**

Abstract: *The most pressing challenges for light-driven hydrogel actuators include reliance on UV light, slow response, poor mechanical properties, and limited functionalities. Now, a supramolecular design strategy is used to address these issues. Key is the use of a benzylimine-functionalized anthracene group, which red-shifts the absorption into the visible region and also stabilizes the supramolecular network through π–π interactions. Acid–ether hydrogen bonds are incorporated for energy dissipation under mechanical deformation and maintaining hydrophilicity of the network. This double-crosslinked supramolecular hydrogel developed via a simple synthesis exhibits a unique combination of high strength, rapid self-healing, and fast visible-light-driven shape morphing both in the wet and dry state. As all of the interactions are dynamic, the design enables the structures to be recycled and reprogrammed into different 3D objects.*

Introduction

Dynamic shape-changing materials are critical to enable function, particularly in a biological context; from muscle contractions to the programmed movement of plants.[1] Light is an ideal stimulus to trigger the shape transformation of materials. Light permits remote, precise manipulation with spatial and temporal control.[2] By tuning various irradiation parameters such as light intensity, exposure time and wavelength, the degree of light-induced bending deformations can be well-controlled.[2a,3] Furthermore, well-defined and complex three-dimensional (3D) structures can be generated through patterned light irradiation[2d,4] or modulating polarization direction.[5] Light-driven actuation enables practical applications in diverse fields such as soft robots,[1f,6] microfluidics,[7] biomedical[8] and optical devices,[9] energy harvesting[10] and manipulation of fluid slugs.[11]

Photoresponsive soft actuators are primarily based on liquid crystal elastomers,[2g,5a,11,12] hydrogels,[2a,b,13] shape memory polymers,[14] crystalline,[15] and carbon-based soft materials.[16] Among these materials, hydrogels are ideal candidates to be developed for this purpose owing to their excellent biocompatibility and similar physiochemical properties to biological soft tissues.[17] Integrating photoactive moieties such as azobenzene,[13a,18] spirobenzopyran,[7] nitrobenzyl,[8,19] stilbene,[20] 4-acetoxystyrene,[21] molecular motors,[22] and photoredox catalysis[23] are widely used approaches to render a hydrogel light-responsive. The molecular conformational change caused by photochemical reactions upon light irradiation could alter solvation properties of the network, triggering macroscopic dimensional changes of the materials. However, despite the progress made in achieving light-induced shape changing hydrogels, many significant issues remain as impediments to application. Most systems use high intensity short-wavelength UV light.[2h] Moreover, the photoresponsive hydrogels typically suffer from poor mechanical properties, namely fatigue-related failure. The hydrogel properties are unable to be recovered or repaired after being damaged. Most designs have permanent crosslinkers hence rendering the hydrogels impossible to be reprocessed or recycled. There is a need for new soft actuators triggered by long-wavelength visible light, which possess diverse functionalities including high mechanical strength, self-healing and recyclability. However, it remains a huge challenge because these material properties are usually realized by different molecular design strategies. Moreover, the introduction of new functionality could come at the cost of another desired property, for example high strength and self-healing are usually opposing properties.[24]

Herein, we report a simple but efficient molecular design strategy to synergistically integrate the above-mentioned properties into a light-driven hydrogel actuator. The key to achieving this is the rational design of the photoactive and dynamic polymeric network based on supramolecular motifs.[25] First, we demonstrated an anthracene small molecule functionalized with a benzyl imine group at the 9-position could induce a red-shift in the absorption and also enhance the photochemical reactivity. The photo-responsive hydrogel was fabricated by covalently incorporating this anthracene small molecule into a soft, flexible, and highly hydrophilic copolymer containing acid–ether hydrogen bonding. The anthracene group was demonstrated to enable the formation of a stable supramolecular network in aqueous solution, significantly enhancing the mechanical properties of hydrogel due to π–π interaction as a crosslinking point. Moreover, the fast visible-light-initiated photo-dimerization of anthracene results in a change in the network properties and thus initiates

[*] Dr. Z. Jiang, M. L. Tan, Dr. Q. Yan, Dr. M. G. Gardiner, B. Diggle, Prof. L. A. Connal
Research School of Chemistry, Australian National University
Canberra, ACT 2601 (Australia)
E-mail: luke.connal@anu.edu.au
M. Taheri, Prof. T. Tsuzuki
Research School of Electrical, Energy, and Materials Engineering, Australian National University
Canberra, ACT 2601 (Australia)
Supporting information and the ORCID identification number(s) for the author(s) of this article can be found under: https://doi.org/10.1002/anie.201916058.

These are not the final page numbers!

rapid actuation both in wet and dry state. Our photoresponsive hydrogel is observed to manifest all the targeted attributes, namely, high mechanical strength, rapid self-healing, self-recovery, fast visible light driven actuation and recyclability. This new molecular design strategy offers the potential to address the limits of the current generation of light-responsive shape changing hydrogels.

Results and Discussion

Material Design and Characterization

Our first aim was to design and synthesize a photochrome molecule that features fast and efficient photochemistry and visible light sensitivity with a relatively simple structure and straightforward synthesis. Anthracene, consisting of three fused benzene rings, came to our attention.[26] It undergoes efficient and reversible photodimerization upon light irradiation, which is expected to tune the swelling ratio of network.[27] The absorption maxima could be red-shifted by placing an electron-rich group at the 9-position of the anthracene ring.[28] Inspired by these examples, we selected anthracene to impart photoresponsiveness into the hydrogel network. The electron-rich imine bond was introduced to functionalize the anthracene ring (Figure 1 A) as it could be readily formed through scalable and simple Schiff base chemistry (Supporting Information, Scheme S1). The synthesis of anthracene small organic molecule was readily achieved by a one-step reaction between commercially available anthracene-9-carbaldehyde and 4-aminophenol. The presence of benzyl substituent on the imine bond was used to enhance the photosensitivity of anthracene under visible-light irradiation for promoting a fast actuation response.[28a] The high purity of the synthesized benzyl imine-functionalized anthracene (BIFA) was confirmed by NMR (Supporting Information, Figure S1). The X-ray single crystal structure of BIFA shows intermolecular face–face π–π stacking interactions between anthracenyl units of 3.43 and 3.58 Å (Supporting Information, Figure S2). UV/Vis spectra of BIFA shows a strong absorption in the visible light region between 400 nm and 470 nm (Supporting Information, Figure S3), which is in contrast with other reported anthracene molecules that only absorbs strongly in UV light region.[27,29]

A key feature of our molecular design is the presence of a hydroxy group in the BIFA, which could be further utilized to covalently attach to polymer chains. We selected poly(-methacrylic acid-*co*-oligo(ethylene glycol) methacrylate)

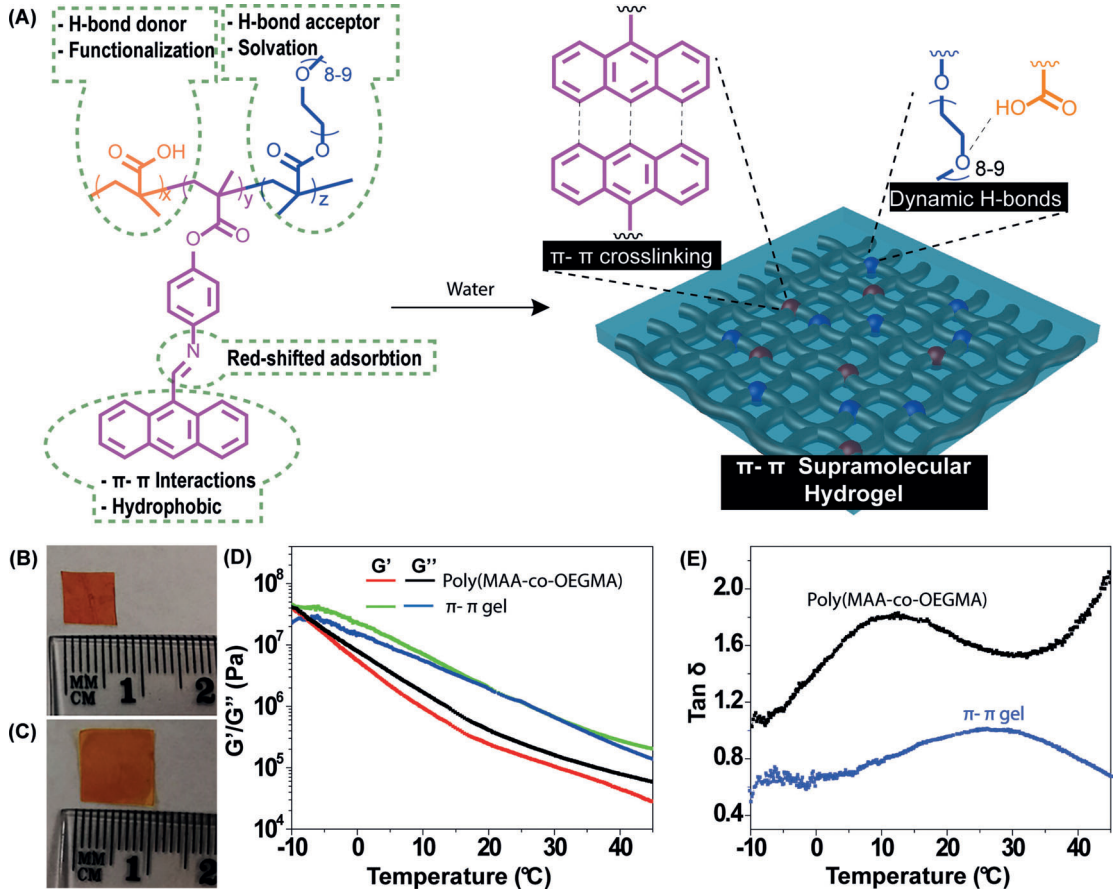

Figure 1. Design and fabrication of a supramolecular photo-responsive hydrogel. A) Chemical structure of supramolecular hydrogel and functions of each rationally designed chemical groups. B),C) Photographs of gels: B) dry π–π gel and C) equilibrium swollen hydrogel with 213 ± 7% water content. D) Temperature dependence of the storage modulus G' and loss modulus G''. E) The loss factor $\tan\delta$ of poly(MAA-*co*-OEGMA) and the π–π gel.

(poly(MAA-*co*-OEGMA) synthesized by one-pot reversible addition-fragmentation chain transfer (RAFT)) polymerization as the polymer matrix. Characterization via NMR indicates a final composition of poly(MAA_{140}-*co*-$OEGMA_{99}$) and $M_n = 51{,}000\ g\,mol^{-1}$. This was chosen due to highly dynamic nature of acid–ether hydrogen bonding,[30] the strong solvation effect of OEGMA,[21,31] while the COOH functional group enables further post-polymerization functionalization. The desired H-bonding interactions in poly(MAA-*co*-OEGMA) were evaluated using FTIR. The carbonyl (C=O) stretching at 1700 cm^{-1} and 1725 cm^{-1} were observed (Supporting Information, Figure S4), which could be ascribed to self-associated COOH dimer and intermolecular hydrogen bond between MAA and OEGMA, respectively.[30] The stronger signal intensity observed at 1725 cm^{-1} compared to that at 1700 cm^{-1} may suggest that most of the MAA units have formed intermolecular hydrogen bond acid–ether hydrogen bonds with OEGMA. The poly(MAA-*co*-OEGMA) was functionalized with BIFA through simple esterification. NMR indicated the successful incorporation of BIFA as confirmed by the presence of broad characteristic peaks of anthracene rings ranging from 6.8 to 9.8 ppm (Supporting Information, Figure S5). The conversion of COOH group into aromatic ester was calculated to be 28 % hence a composition of poly(MAA_{140}-*co*-$BIFA_{39}$-*co*-$OEGMA_{60}$). π–π stacking in the functionalized copolymer was confirmed by the red-shifted absorbance compared to that of BIFA small molecule (Supporting Information, Figure S6).

To understand the role of anthracene functionality on physicochemical properties of the network, first, the stability of poly(MAA-*co*-OEGMA) and BIFA functionalized poly(-MAA-*co*-OEGMA) in water were investigated. As shown in the Supporting Information, Figure S7, the poly(MAA-*co*-OEGMA) was observed to be dissolved after being immersed in water for 24 h, which could be explained as highly water solubility of the OEGMA unit. In contrast, BIFA functionalized poly(MAA-*co*-OEGMA) soaked in water was insoluble but only swollen and lead to an eventual equilibrium degree (Figure 1 B,C). Such substantial difference could be ascribed to the strong π–π interaction in the anthracene copolymer as additional supramolecular crosslinking sites as well as enhanced intermolecular hydrogen bonds by the increased hydrophobic environment.[32] The observed broad −O−H stretching vibrations from 3300–3600 cm^{-1} and the new strong peak at 1640 cm^{-1} in FTIR demonstrate (Supporting Information, Figure S8) stretching vibrations of hydrogen bond between ester carbonyl groups and water. It is worth noting that the peak at 1725 cm^{-1} ascribed to the intermolecular hydrogen bond between MAA and OEGMA could still be detected even in the wet state, indicating the presence of acid–ether hydrogen bonds stabilized by a hydrophobic methyl motif and anthracene group. The equilibrium water content was measured to be as high as 213 ± 7 % despite a relatively high content of hydrophobic anthracene group, which could be interpreted as a result of solvation effect offered by the relatively long oligo(ethylene glycol) side chain.[21,31] This result illustrates that the incorporation of an anthracene group could facilitate the formation of stable supramolecular hydrogel network in water without the need to use covalent crosslinkers which have been commonly employed in fabricating other photoresponsive hydrogels.[13,18b] To simplify discussion, the BIFA functionalized poly(MAA-*co*-OEGMA) will be referred to as π–π hydrogel.

The π–π hydrogel was further analyzed via dynamic mechanical analyzer (DMA). The temperature sweep showed an increase of 9 orders of magnitude in the storage modulus for the π–π hydrogel compared to that of poly(MAA-*co*-OEGMA) at 25 °C (Figure 1 D). The lower $\tan\delta$ of the π–π hydrogel is indicative of an increased elastic character[33] as a result of anthracene incorporation. The frequency sweep at room temperature revealed that the storage modulus (G') of poly(MAA-*co*-OEGMA) is consistently lower than that of loss modulus (G'') over the frequency range (Supporting Information, Figure S9 A), implying that the polymer is in liquid state. However, the π–π hydrogel showed a crossover where $G' = G''$ at frequency of 12 $rad\,s^{-1}$ (Supporting Information, Figure S9 B) and G' was greater than G'' at higher frequencies, indicating more solid like properties. These results confirm that the anthracene group plays an important role in stabilizing hydrogel network through forming additional π–π crosslinking.[34]

Mechanical and Self-Healing Properties

One of the major challenges that restricts widespread use of hydrogel actuators in many applications is their poor mechanical properties. The material design concept in this work could allow high mechanical strength and toughness, which is enabled by the π–π and hydrogen-bonding crosslinked networks. The weak acid–ether hydrogen bonding could efficiently dissipate energy by bond scission, while the stronger π–π interactions can withstand mechanical forces to maintain the integrality of network.[35] The robust mechanical properties of the hydrogel (4 × 1 × 0.08 cm) was demonstrated as the ability to withstand 3000 × its own weight (Figure 2 A). The hydrogel could also be bent and twisted into a helical shape without failure (Figure 2 A). The anthracene incorporation in the polymer networks brings about a 11-fold increase in Young's modulus and a 20-fold increase in tensile strength from 0.18 ± 0.02 to 3.67 ± 0.02 MPa. This change also comes with a decrease in the stretching ratio because of reinforced interchain interaction and rigidity (Figure 2 B). The π–π hydrogel displayed remarkable physical properties for a non-covalent material, including high fracture stress (3.7 ± 0.4 % MPa) and Young's modulus (10 MPa), toughness (6.6 ± 0.1 % $MJ\,m^{-3}$) and fracture strain (353 ± 4 %). The Young's modulus of this hydrogel is hundreds of times higher than other reported photochemically shape changing hydrogels (Young's modulus ca. 8.5 kPa to 45 kPa).[18b,c,19,20,23a] While in contrast, the poly(MAA-*co*-OEGMA) lacking π–π interaction was observed to be a soft, tacky film measured with circa 0.1 MPa tensile stress and low Young's modulus of 0.9 MPa and could not be fractured even after stretching over 8000 % of its original size (Figure 2 B). Furthermore, stress-relaxation measurements showed remarkable longer relaxation time τ and only 18 % of released stress in supramolecular hydrogel (Supporting Information, Figure S10). The resisted complete

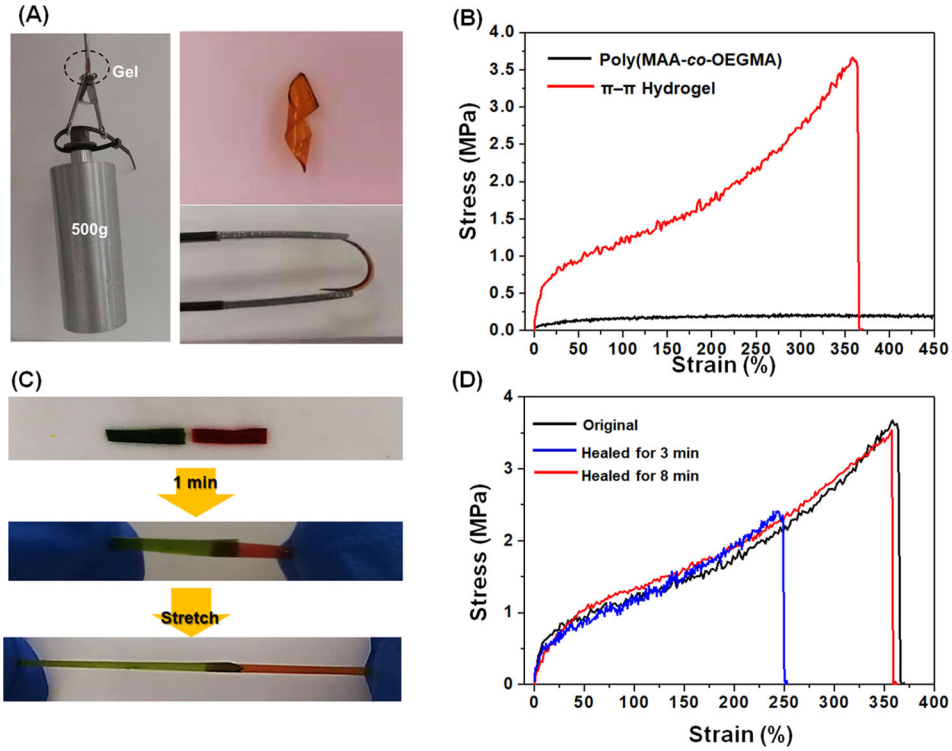

Figure 2. Mechanical and self-healing properties of the π–π hydrogel. A) Photographs of the hydrogel, which could lift heavy objects and also be easily twisted and curved. B) Stress–strain curves of poly(MAA-*co*-OEGMA) and π–π hydrogel demonstrating the improved properties through the anthracene functionalization. C) Photographs showing qualitative evidence of self-healing; after healing for 1 min the gels could be stretched to 100%. D) Quantitative evidence for self-healing comparing the stress–strain curves for original and healed π–π hydrogel samples after different healing times at 35 °C.

stress relaxation could originate from the strong and dense π–π stacking as efficient crosslinking sites. These results demonstrate the importance of π–π interaction from anthracene, which has considerably higher dissociation energies and much slower relaxation time than hydrogen bonds,[35a] in strengthening the networks and increasing the intermolecular interaction. We also performed a loading–unloading test of π–π hydrogel at a maximal strain of 100% (Supporting Information, Figure S11). The observed large prominent hysteresis loops for strains beyond the linear regime indicates efficient energy dissipation which could be ascribed to the rupture of sacrificial hydrogen bonding. The hysteresis loop recovered to its original value after a waiting time of 20 min. This result indicates the fast and efficient self-recovery properties of our hydrogel, which could be as a result of fast reassociation of the broken hydrogen bonding and elasticity provided by π–π interaction of the anthracene group.[35a]

Self-healing can also be engineered into this system as the material consists of non-covalent interactions that are generally under continuous equilibrium.[36] We assessed the self-healing properties of the hydrogel by attaching two hydrogel slabs with different colors at 35 °C. The hydrogel was in elastomeric state at 35 °C, which could promote the dissociation and reform of π–π interaction and hydrogen bonding (Figure 1 D,E). After only 1 min, the hydrogel interface became so tightly attached that it still maintained integrity after further stretch up to elongation of 100% (Figure 2 C). We then designed experiments to isolate each dynamic bond independently to establish if both are responsible for self-healing. To isolate the π–π bonds, two cut edges were dipped in *t*-butanol, which could break the acid–ether hydrogen bonding,[37] brought in contact, and heated at 35 °C for 3 min (Supporting Information, Figure S12 A). The cut surfaces of the two separate pieces were tightly merged, which could be ascribed to the π–π bond reforming. To isolate the hydrogen bonding, the self-healing property was studied in THF, which breaks the π–π bond in anthracene.[38] Following the same procedure it can be seen that the two separate pieces could still be fused together within 3 min (Supporting Information, Figure S12 B), which could be attributed to the highly dynamic acid-ether hydrogen bonding. These results indicate that both π–π and hydrogen bonds contribute to the self-healing properties.

Tensile testing was then conducted to quantitatively study self-healing properties. It was shown that the π–π hydrogel exhibited a rapid self-healing at 35 °C, and 68% recovery of the original fracture stress was observed after only 3 min. An almost complete overlap with original curve is possible after only 8 min (Figure 2 D). As self-healing is related to polymer chain relaxation dynamics, the frequency sweep of hydrogel at 35 °C was tested. As shown in the Supporting Information, Figure S13, the relaxation time of hydrogel was calculated to be 0.007 s, using the reciprocal of the crossover angular frequency. This calculated chain relaxation time is comparable to that of other ultra-fast self-healing polymers.[30,39] These results indicate that the excellent self-healing could be

ascribed to fast chain mobility and dynamic exchange of noncovalent bonds in the π–π hydrogel.

Photoresponsive Shape Changing Behavior

Besides enhancing mechanical properties through π-π crosslinking, the anthracene group could undergo the photocrosslinking reaction. We anticipated this to change the microscopic network swelling degree and induce a macroscopic shape change. The photochemical process of π–π hydrogel was followed by UV/Vis spectra (Figure 3 A). It was observed that irradiation of the hydrogel thin film with visible light (420–530 nm, 10 mW cm^{-1}) resulted in rapid reduction of the absorption peak from 400 nm and 470 nm, indicating the dimerization of anthracene. Assuming first order reaction kinetics, the dimerization rate constants for hydrogel was calculated to be 1.6×10^{-3} s^{-1}, which is comparable to that of the aromatic triazole ring substituted anthracene that was used for fast gelation process.[28a] This result reveals that our π–π hydrogel not only shows visible light responsiveness, but also fast photochemical kinetics. Furthermore, the FTIR spectral of exposed hydrogel showed the appearance of new peak at 765 cm^{-1} which could be ascribed to the anthracene dimer signal (Supporting Information, Figure S14).[29c] Moreover, the loss of signal at 1625 cm^{-1} corresponding to the imine bond may suggest the occurring of [4+2] Diels–Alder photocycloaddition.[26a,40]

We then investigated the changes in the properties of hydrogels under visible light irradiation. The equilibrium water content of irradiated hydrogel is lower than that of its original content (Supporting Information, Figure S15), suggesting the reduced hydration of the network. The visible-light irradiation was also shown to result in a significant increase in tensile strengths and Young's moduli (Supporting Information, Figure S16), reflecting the crosslinking of the hydrogel network owing to photodimerization of anthracene. Further heating the exposed hydrogel at 90 °C for 0.5 h almost restored the tensile curve of the hydrogel back to the unexposed state, which could be ascribed to the thermally induced reversibility of the of anthracene photodimerization, confirmed by FTIR results (Supporting Information, Figure S14).

The absorption coefficient of this newly designed anthracene group is as large as 1.65×10^4 (Supporting Information, Figure S3), suggesting that the top layer with a thickness of 2 μm absorbs 99 % of the incident visible light and generate a structural gradient across the hydrogel thickness.[3c,12d] To verify this, exposed π–π hydrogel was then studied by various methods, including UV/Vis spectroscopy, Fourier-transform infrared spectroscopy (FTIR), and scanning electron microscopy (SEM). The transmittance of hydrogel film (20 μm thickness) was studied by UV/Vis spectroscopy (Supporting Information, Figure S17). It was found that the light transmittance from 350 nm to 500 nm is only 12 %. Moreover, structural characterization of the top and bottom surface

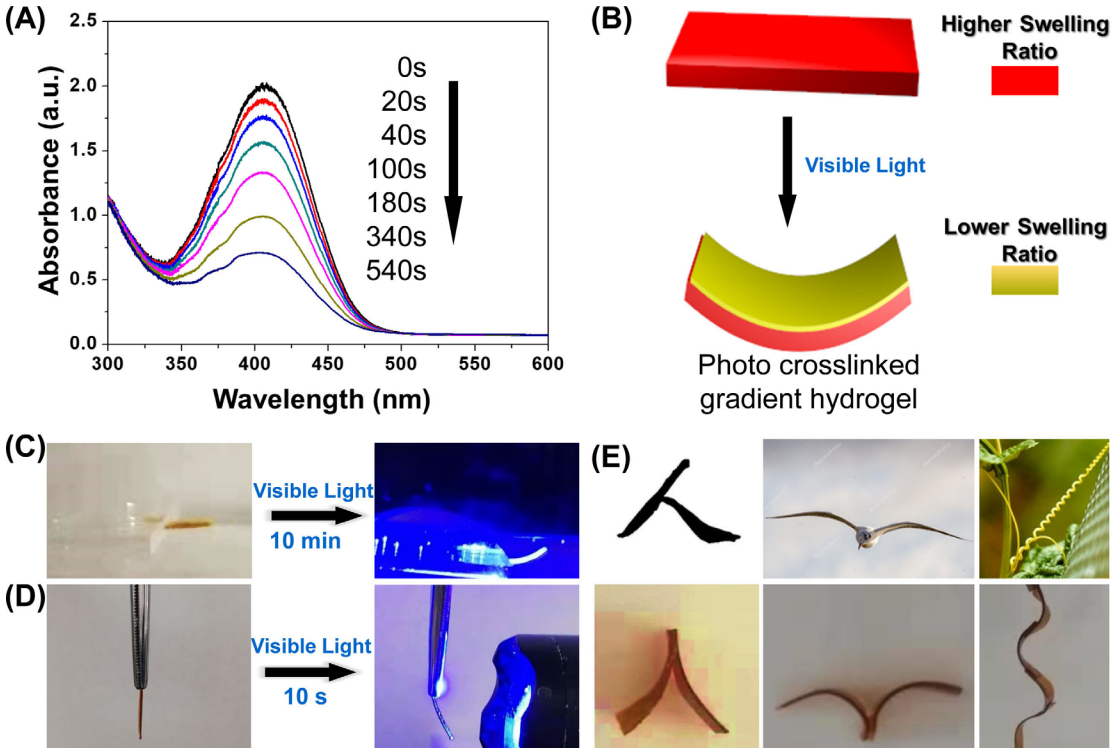

Figure 3. Photoresponsive behaviors of π–π hydrogels. A) UV/Vis spectra of the π–π hydrogel (thickness ca. 20 μm) under visible-light irradiation (420–530 nm, 10 mW cm^{-1}). B) Illustration showing the formation of photo crosslinked hydrogel with a gradient in the crosslink density. The different network creates a different swelling ratio across the hydrogel and creates a bending moment toward the light source when irradiated. C),D) Photographs of the hydrogel bending toward the light source upon visible light irradiation in water (C) and dry state (D). E) Various complex 3D morphologies achieved through joining the shape programed dry hydrogels.

indicated different chemical compositions (Supporting Information, Figure S18), the anthracene dimer signal was not observed in the unexposed bottom side. SEM results showed that the cross-section consists of a rough and heterogeneous surface structure caused by lower crosslinking density. In regions of higher crosslink density a smoother more uniform surface structure was observed (Supporting Information, Figure S19).[41] These results confirm the formation of a gradient across the hydrogel with more photodimerization at the top surface and very little dimerization at the bottom surface.

The light-programmed gradient in crosslinking density could translate into macroscopic 3D bending motion. As shown in the Supporting Information, Figure S20, the swollen hydrogel ($3 \times 0.7 \times 0.1$ cm) bent toward the light source side in water, reaching a bending angle of 12° after irradiation of 1 h. Similar phenomenon has been observed in other photoswitchable hydrogels.[13a,18b] The exposed surface of the hydrogel preferentially absorbs the light energy and has a much lower swelling ratio compared to the regions away from the light sources. Furthermore, the excellent mechanical properties of our materials enabled fabrication of thinner films (thickness ca. 80 μm) without breakage, which exhibited much faster response speed with bending angle of 15° after only 10 mins (Figure 3C). This could be interpreted as a result of a faster water diffusion process in thinner hydrogel film.[42]

We then investigated the photoinduced actuation behavior in a dry double crosslinked polymer without water uptake. Taking advantage of high stretchability, initially, the gel was uniaxially elongated to a strain of 157% without being fractured. When this force was removed, the gel would slowly recover to this original length within 20 min due to excellent elasticity imparted by π–π crosslinking (Supporting Information, Figure S21). Interestingly, irradiating the prestretched gel generated rapid bending toward the light source (Supporting Information, Movie 1) with a bending angle of 28° within 20 s (Figure 3D). And bending angle increased with the increase in irradiation time and finally reached a stable bending state (Supporting Information, Figure S22A). There results indicate that our polymeric actuators could be working in different environments. The photoinduced bending movement in dry gel comes from the enhanced elastic recovery process[43] in the irradiated side owing to slightly increased chemical crosslinking density upon light irradiation. The bent film reverted to the initial flat state within 60 min when heated to 90°C (Supporting Information, Figure S22C) the associated cleavage of the anthracene dimers was confirmed by UV/Vis (Supporting Information, Figure S22B) and FTIR spectral results (Supporting Information, Figure S14). The reversible shape transformation could be cycled at least 5 times without obvious change in performance (Supporting Information, Figure S22D).

Furthermore, combining the excellent self-healing properties enables the fabrication of a variety of complex 3D morphologies simply through conjoining the actuated gel slabs. As shown in Figure 3E, when the two deformed hydrogel with bending angle of 21° were assembled by joining the edges, a Chinese character "人" was created. The 3D shape mimicking a flying bird could be afforded through assembling the two actuated gel slabs with larger bending angle of 38° in a similar manner. Furthermore, we obtained a cucumber tendril like shape through combining 4 actuated hydrogels with bending angle of 31° at both ends.

Light-responsive shape-changing hydrogels were usually constructed with covalent crosslinkers.[2a,13a,18b,c,20] Once the 3D shape deformations of the photoresponsive hydrogel have been generated, these cannot be recycled. Our molecular design concept for constructing light-responsive hydrogel actuators is based on multiple dynamic chemistries and thus enables new possibilities in recycling. To demonstrate this, a helical structure was produced through selectively exposing a dry hydrogel sheet with a stripe angle of 45° followed by immersing in water (Figure 4A,B). This actuated hydrogel was able to be dissolved in DMF which is a good solvent for both anthracene and poly(MAA-*co*-OEGMA) while being heated at temperature of 90°C (Figure 4C) because the anthracene dimerization is thermally reversable (Supporting Information, Figure S14). In contrast, the actuated hydrogel could not be dissolved by directly mixing with DMF without heat treatment (Supporting Information, Figure S23). The dissolved polymer solution was further remoulded into a cross

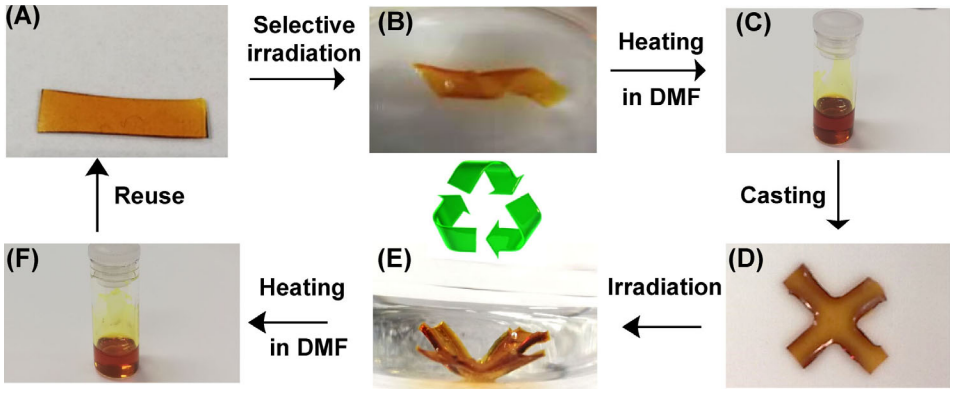

Figure 4. Photographs showing the recycle and reprogrammable process of π–π hydrogel. A) the original as cast film. B) Helical structure was formed by patterned light irradiation with strip angle of 45° after immersion in water. C) The hydrogel could be re-dissolved in DMF with heat. D) The hydrogel can be recast into a new shape. E) The new 3D shape morphology was obtained through light irradiation. F) The hydrogel can be further re-processed by dissolving in DMF at 90°C.

geometry through solution casting (Figure 4D). The shape mimicking flower bloom could be achieved by uniformly light irradiation followed by immersing in water (Figure 4E). The actuated flower shape hydrogel was re-dissolved into hot DMF solution (Figure 4F) which could be further reused for fabricating other 3D geometries.

Conclusion

We have succeeded in developing a new class of photoresponsive shape-changing hydrogels through rational design of multiple dynamic chemistries. To achieve a supramolecular double network hydrogel, a red-shifted anthracene derivative was covalently incorporated into an engineered copolymer of poly(MAA-*co*-OEGMA). The introduction of anthracene performs multiple tasks; it effectively promotes the formation of stable supramolecular network in water, significantly reinforcing the mechanical strength owing to strong π–π interactions. The red-shifted anthracene also enables the system to undergo fast photodimerization process upon visible light irradiation. Our supramolecular polymer design strategy facilitates the integration of a number of superior material properties synergistically in a single light-responsive shape changing hydrogel. We demonstrate visible-light-driven and fast deformation both in wet and dry states, high mechanical strength, self-healing, self-recovery, and also the capability of being recyclable and reprogrammable. We would like to highlight the simple molecular structure and ease of synthesis of this system. This innovative molecular design concept has addressed the most critical limitations in traditional light-driven hydrogel actuators and is expected to promote practical applications of this type of materials in various fields. Importantly, this work not only is a significant step forward to develop a novel light-controllable hydrogel but also represents a new strategy on the technological applications of photoresponsive anthracene in smart hydrogel devices.

Acknowledgements

Funding is gratefully acknowledged from the Australian Research Council (DP180103918), and the ANU Futures Scheme. Z.J. would like to acknowledge funding of ANU Early Career Researchers (ECR) Travel Grant (R.46850.4656). The authors would like to thank Prof. Yanlei Yu for constructive discussions on the mechanism of photo-induced bending in dry gels. The authors thank Associate Professor Zbigniew Stachurski for assistance with tensile testing. The authors also acknowledge the facilities and the scientific and technical assistance of Microscopy Australia at the Advanced Imaging Precinct, Australian National University, a facility that is funded by the University, and State and Federal Governments.

Conflict of interest

The authors declare no conflict of interest.

Keywords: actuators · anthracene · photoresponsive hydrogels · self-healing

[1] a) H. Ko, A. Javey, *Acc. Chem. Res.* **2017**, *50*, 691 – 702; b) S. M. Mirvakili, I. W. Hunter, *Adv. Mater.* **2018**, *30,* 1704407; c) S. Poppinga, C. Zollfrank, O. Prucker, J. Ruhe, A. Menges, T. Cheng, T. Speck, *Adv. Mater.* **2018**, *30*, 1703653; d) E. Siefert, E. Reyssat, J. Bico, B. Roman, *Nat. Mater.* **2019**, *18*, 24 – 28; e) A. Miriyev, K. Stack, H. Lipson, *Nat. Commun.* **2017**, *8*, 596; f) G. M. Whitesides, *Angew. Chem. Int. Ed.* **2018**, *57*, 4258 – 4273; *Angew. Chem.* **2018**, *130*, 4336 – 4353.

[2] a) G. Stoychev, A. Kirillova, L. Ionov, *Adv. Opt. Mater.* **2019**, *7*, 1900067; b) L. Li, J. M. Scheiger, P. A. Levkin, *Adv. Mater.* **2019**, *31*, 1807333; c) E. Blasco, M. Wegener, C. Barner-Kowollik, *Adv. Mater.* **2017**, *29,* 1604005; d) D. D. Han, Y. L. Zhang, J. N. Ma, Y. Q. Liu, B. Han, H. B. Sun, *Adv. Mater.* **2016**, *28*, 8328 – 8343; e) Z. Jiang, Y. Xiao, X. Tong, Y. Zhao, *Angew. Chem. Int. Ed.* **2019**, *58*, 5332 – 5337; *Angew. Chem.* **2019**, *131*, 5386 – 5291; f) J. del Barrio, C. Sánchez-Somolinos, *Adv. Opt. Mater.* **2019**, *7*, 1900598; g) B. Zuo, M. Wang, B. P. Lin, H. Yang, *Nat. Commun.* **2019**, *10*, 4539; h) J. Boelke, S. Hecht, *Adv. Opt. Mater.* **2019**, *7*, 1900404.

[3] a) T. Ikeda, J. i. Mamiya, Y. Yu, *Angew. Chem. Int. Ed.* **2007**, *46*, 506 – 528; *Angew. Chem.* **2007**, *119*, 512 – 535; b) A. H. Gelebart, D. J. Mulder, G. Vantomme, A. Schenning, D. J. Broer, *Angew. Chem. Int. Ed.* **2017**, *56*, 13436 – 13439; *Angew. Chem.* **2017**, *129*, 13621 – 13624; c) M. Chen, B. Yao, M. Kappl, S. Liu, J. Yuan, R. Berger, F. Zhang, H. J. Butt, Y. Liu, S. Wu, *Adv. Funct. Mater.* **2020**, *30*, 1906752.

[4] a) Y. Dong, J. Wang, X. Guo, S. Yang, M. O. Ozen, P. Chen, X. Liu, W. Du, F. Xiao, U. Demirci, B. F. Liu, *Nat. Commun.* **2019**, *10*, 4087; b) A. Ryabchun, Q. Li, F. Lancia, I. Aprahamian, N. Katsonis, *J. Am. Chem. Soc.* **2019**, *141*, 1196 – 1200; c) C. Y. Li, X. P. Hao, Z. L. Wu, Q. Zheng, *Chem. Asian J.* **2019**, *14*, 94 – 104.

[5] a) Y. Yu, M. Nakano, T. Ikeda, *Nature* **2003**, *425*, 145; b) T. J. White, N. V. Tabiryan, S. V. Serak, U. A. Hrozhyk, V. P. Tondiglia, H. Koerner, R. A. Vaia, T. J. J. S. M. Bunning, *Soft Matter* **2008**, *4*, 1796 – 1798.

[6] a) B. Jin, H. Song, R. Jiang, J. Song, Q. Zhao, T. Xie, *Sci. Adv.* **2018**, *4*, eaao3865; b) H. Zeng, P. Wasylczyk, D. S. Wiersma, A. Priimagi, *Adv. Mater.* **2018**, *30*, 1703554.

[7] J. ter Schiphorst, S. Coleman, J. E. Stumpel, A. Ben Azouz, D. Diamond, A. P. H. J. Schenning, *Chem. Mater.* **2015**, *27*, 5925 – 5931.

[8] E. Käpylä, S. M. Delgado, A. M. Kasko, *ACS Appl. Mater. Interfaces* **2016**, *8*, 17885 – 17893.

[9] a) N. J. Dawson, M. G. Kuzyk, J. Neal, P. Luchette, P. Palffy-Muhoray, in *Liquid Crystals XVI, Vol. 8475*, International Society for Optics and Photonics, **2012**, p. 84750B; b) Z. Yan, X. Ji, W. Wu, J. Wei, Y. Yu, *Macromol. Rapid Commun.* **2012**, *33*, 1362 – 1367; c) O. M. Wani, H. Zeng, A. Priimagi, *Nat. Commun.* **2017**, *8*, 15546; d) C. Boott, A. Tran, W. Hamad, M. MacLachlan, *Angew. Chem. Int. Ed.* **2020**, *59*, 226 – 231; *Angew. Chem.* **2020**, *132*, 232 – 237.

[10] G. Vantomme, A. Gelebart, D. Broer, E. Meijer, *Tetrahedron* **2017**, *73*, 4963 – 4967.

[11] J.-a. Lv, Y. Liu, J. Wei, E. Chen, L. Qin, Y. Yu, *Nature* **2016**, *537*, 179.

[12] a) T. Ube, K. Kawasaki, T. Ikeda, *Adv. Mater.* **2016**, *28*, 8212 – 8217; b) T. Ube, T. Ikeda, *Adv. Opt. Mater.* **2019**, *7*, 1900380; c) Z. Jiang, M. Xu, F. Li, Y. Yu, *J. Am. Chem. Soc.* **2013**, *135*, 16446 – 16453; d) X. Pang, J.-a. Lv, C. Zhu, L. Qin, Y. Yu, *Adv. Mater.* **2019**, *31*, 1904224; e) F. Ge, R. Yang, X. Tong, F. Camerel, Y. Zhao, *Angew. Chem. Int. Ed.* **2018**, *57*, 11758 – 11763; *Angew. Chem.* **2018**, *130*, 11932 – 11937.

[13] a) Y. Takashima, S. Hatanaka, M. Otsubo, M. Nakahata, T. Kakuta, A. Hashidzume, H. Yamaguchi, A. Harada, *Nat. Commun.* **2012**, *3*, 1270; b) M. Mauro, *J. Mater. Chem. B* **2019**, *7*, 4234 – 4242.

[14] a) C. Löwenberg, M. Balk, C. Wischke, M. Behl, A. Lendlein, *Acc. Chem. Res.* **2017**, *50*, 723 – 732; b) D. Habault, H. Zhang, Y. Zhao, *Chem. Soc. Rev.* **2013**, *42*, 7244 – 7256.

[15] Q. Yu, X. Yang, Y. Chen, K. Yu, J. Gao, Z. Liu, P. Cheng, Z. Zhang, B. Aguila, S. Ma, *Angew. Chem. Int. Ed.* **2018**, *57*, 10192 – 10196; *Angew. Chem.* **2018**, *130*, 10349 – 10353.

[16] M. Yang, Z. Yuan, J. Liu, Z. Fang, L. Fang, D. Yu, Q. Li, *Adv. Opt. Mater.* **2019**, *7*, 1900069.

[17] a) X. Le, W. Lu, J. Zhang, T. Chen, *Adv. Sci.* **2019**, *6*, 1801584; b) O. Erol, A. Pantula, W. Liu, D. H. Gracias, *Adv. Mater. Technol.* **2019**, *4*, 1900043.

[18] a) J. Wei, Y. Yu, *Soft Matter* **2012**, *8*, 8050 – 8059; b) K. Iwaso, Y. Takashima, A. Harada, *Nat. Chem.* **2016**, *8*, 625 – 632; c) Y. Takashima, Y. Hayashi, M. Osaki, F. Kaneko, H. Yamaguchi, A. Harada, *Macromolecules* **2018**, *51*, 4688 – 4693.

[19] Y. Liao, N. An, N. Wang, Y. Zhang, J. Song, J. Zhou, W. Liu, *Macromol. Rapid Commun.* **2015**, *36*, 2129 – 2136.

[20] S. Ikejiri, Y. Takashima, M. Osaki, H. Yamaguchi, A. Harada, *J. Am. Chem. Soc.* **2018**, *140*, 17308 – 17315.

[21] Z. Jiang, R. J. P. Sanchez, I. Blakey, A. K. Whittaker, *Chem. Commun.* **2018**, *54*, 10909 – 10912.

[22] J. Chen, F. K. Leung, M. C. A. Stuart, T. Kajitani, T. Fukushima, E. van der Giessen, B. L. Feringa, *Nat. Chem.* **2018**, *10*, 132 – 138.

[23] a) F. Amir, K. P. Liles, A. O. Delawder, N. D. Colley, M. S. Palmquist, H. R. Linder, S. A. Sell, J. C. Barnes, *ACS Appl. Mater. Interfaces* **2019**, *11*, 24627 – 24638; b) K. P. Liles, A. F. Greene, M. K. Danielson, N. D. Colley, A. Wellen, J. M. Fisher, J. C. Barnes, *Macromol. Rapid Commun.* **2018**, *39*, 1700781.

[24] A. Lendlein, M. Balk, N. A. Tarazona, O. E. C. Gould, *Biomacromolecules* **2019**, *20*, 3627 – 3640.

[25] a) T. F. de Greef, E. Meijer, *Nature* **2008**, *453*, 171; b) X. Yan, F. Wang, B. Zheng, F. Huang, *Chem. Soc. Rev.* **2012**, *41*, 6042 – 6065; c) E. A. Appel, J. del Barrio, X. J. Loh, O. A. Scherman, *Chem. Soc. Rev.* **2012**, *41*, 6195 – 6214; d) A. Harada, Y. Takashima, M. Nakahata, *Acc. Chem. Res.* **2014**, *47*, 2128 – 2140; e) M. Nadgorny, Z. Xiao, L. A. Connal, *Mol. Syst. Des. Eng.* **2017**, *2*, 283 – 292; f) Z. Jiang, A. Bhaskaran, H. M. Aitken, I. C. Shackleford, L. A. Connal, *Macromol. Rapid Commun.* **2019**, *40*, 1900038; g) M. Nadgorny, J. Collins, Z. Xiao, P. J. Scales, L. A. Connal, *Polym. Chem.* **2018**, *9*, 1684 – 1692.

[26] a) J. Van Damme, F. Du Prez, *Prog. Polym. Sci.* **2018**, *82*, 92 – 119; b) H. Xie, K.-K. Yang, Y.-Z. Wang, *Prog. Polym. Sci.* **2019**, *95*, 32 – 64.

[27] J. Bai, Z. Shi, J. Yin, M. Tian, R. Qu, *Adv. Funct. Mater.* **2018**, *28*, 1800939.

[28] a) V. X. Truong, F. Li, J. S. Forsythe, *ACS Macro Lett.* **2017**, *6*, 657 – 662; b) T. K. Claus, S. Telitel, A. Welle, M. Bastmeyer, A. P. Vogt, G. Delaittre, C. Barner-Kowollik, *Chem. Commun.* **2017**, *53*, 1599 – 1602.

[29] a) K. A. Günay, T. L. Ceccato, J. S. Silver, K. L. Bannister, O. J. Bednarski, L. A. Leinwand, K. S. Anseth, *Angew. Chem. Int. Ed.* **2019**, *58*, 9912 – 9916; *Angew. Chem.* **2019**, *131*, 10017 – 10021; b) L. A. Connal, R. Vestberg, C. J. Hawker, G. G. Qiao, *Adv. Funct. Mater.* **2008**, *18*, 3315 – 3322; c) T. Hughes, G. P. Simon, K. Saito, *ACS Appl. Mater. Interfaces* **2019**, *11*, 19429 – 19443; d) H. Xie, M.-j. He, X.-Y. Deng, L. Du, C.-J. Fan, K.-K. Yang, Y.-Z. Wang, *ACS Appl. Mater. Interfaces* **2016**, *8*, 9431 – 9439.

[30] J.-L. Hong, P.-N. Song, *J. Mater. Chem. C* **2019**, *7*, 13161 – 13175.

[31] a) Z. Jiang, I. Blakey, A. K. Whittaker, *Polym. Chem.* **2017**, *8*, 4114 – 4123; b) Z. Jiang, H.-H. Cheng, I. Blakey, A. K. Whittaker, *Mol. Syst. Des. Eng.* **2018**, *3*, 627 – 635; c) Z. Jiang, B. Diggle, I. C. G. Shackleford, L. A. Connal, *Adv. Mater.* **2019**, *31*, 1904956.

[32] a) M. Guo, L. M. Pitet, H. M. Wyss, M. Vos, P. Y. Dankers, E. Meijer, *J. Am. Chem. Soc.* **2014**, *136*, 6969 – 6977; b) R. Liang, H. Yu, L. Wang, L. Lin, N. Wang, K. U. Naveed, *ACS Appl Mater Interfaces* **2019**, *11*, 43563 – 43572; c) I. Jeon, J. Cui, W. R. Illeperuma, J. Aizenberg, J. J. Vlassak, *Adv. Mater.* **2016**, *28*, 4678 – 4683; d) Y. J. Wang, X. N. Zhang, Y. Song, Y. Zhao, L. Chen, F. Su, L. Li, Z. L. Wu, Q. Zheng, *Chem. Mater.* **2019**, *31*, 1430 – 1440.

[33] C. Wang, K. Deitrick, J. Seo, Z. Cheng, N. S. Zacharia, R. A. Weiss, B. D. Vogt, *Macromolecules* **2019**, *52*, 6055 – 6067.

[34] L. Chen, H.-B. Zhao, Y.-P. Ni, T. Fu, W.-S. Wu, X.-L. Wang, Y.-Z. Wang, *J. Mater. Chem. A* **2019**, *7*, 17037 – 17045.

[35] a) H. J. Zhang, T. L. Sun, A. K. Zhang, Y. Ikura, T. Nakajima, T. Nonoyama, T. Kurokawa, O. Ito, H. Ishitobi, J. P. Gong, *Adv. Mater.* **2016**, *28*, 4884 – 4890; b) J. Y. Sun, X. Zhao, W. R. Illeperuma, O. Chaudhuri, K. H. Oh, D. J. Mooney, J. J. Vlassak, Z. Suo, *Nature* **2012**, *489*, 133 – 136.

[36] R. J. Wojtecki, M. A. Meador, S. J. Rowan, *Nat. Mater.* **2011**, *10*, 14.

[37] E. C. Goh, H. D. J. M. Stöver, *Macromolecules* **2002**, *35*, 9983 – 9989.

[38] K. Jin, A. Banerji, D. Kitto, F. S. Bates, C. J. Ellison, *ACS Appl. Mater. Interfaces* **2019**, *11*, 12863 – 12870.

[39] a) D.-P. Wang, Z.-H. Zhao, C.-H. Li, J.-L. Zuo, *Mater. Chem. Front.* **2019**, *3*, 1411 – 1421; b) D. L. Taylor, M. In Het Panhuis, *Adv. Mater.* **2016**, *28*, 9060 – 9093.

[40] a) M. Kim, J. N. Hohman, Y. Cao, K. N. Houk, H. Ma, A. K.-Y. Jen, P. S. Weiss, *Science* **2011**, *331*, 1312 – 1315; b) T. Zdobinsky, P. Sankar Maiti, R. Klajn, *J. Am. Chem. Soc.* **2014**, *136*, 2711 – 2714; c) S. Das, N. Okamura, S. Yagi, A. Ajayaghosh, *J. Am. Chem. Soc.* **2019**, *141*, 5635 – 5639.

[41] E. A. Kamoun, A. M. Omer, S. N. Khattab, H. M. Ahmed, A. A. Elbardan, *J. Appl. Pharm. Sci.* **2018**, *8*, 034 – 042.

[42] H. Guo, J. Cheng, J. Wang, P. Huang, Y. Liu, Z. Jia, X. Chen, K. Sui, T. Li, Z. Nie, *J. Mater. Chem. B* **2017**, *5*, 2883 – 2887.

[43] S. Wang, G. Li, Z. Liu, Z. Liu, J. Jiang, Y. Zhao, *ACS Appl. Mater. Interfaces* **2019**, *11*, 30308 – 30316.

Manuscript received: December 15, 2019
Revised manuscript received: January 20, 2020
Version of record online: ■■ ■■, ■■■■

Research Articles

Supramolecular Chemistry

Z. Jiang, M. L. Tan, M. Taheri, Q. Yan, T. Tsuzuki, M. G. Gardiner, B. Diggle, L. A. Connal* _____ ▮▮▮▮–▮▮▮▮

Strong, Self-Healable, and Recyclable Visible-Light-Responsive Hydrogel Actuators

A photoresponsive hydrogel was constructed by using a supramolecular design strategy. A red-shifted anthracene group furnishes the system with fast photo-actuation. Hydrogen bonding, π–π interactions, and anthracene photodimerization results in an actuator with high mechanical strength, fast self-healing, and recyclability.